Acta Crystallographica Section F
Structural Biology and Crystallization Communications
ISSN 1744-3091

Expression, purification, crystallization and preliminary X-ray analysis of *Pseudomonas aeruginosa* PelD

Lindsey S. Marmont,[a] John C. Whitney,[a,b] Howard Robinson,[c] Kelly M. Colvin,[d] Matthew R. Parsek[d] and P. Lynne Howell[a,b]*

[a]Program in Molecular Structure and Function, Research Institute, Hospital for Sick Children, 555 University Avenue, Toronto, ON M5G 1X8, Canada, [b]Department of Biochemistry, Faculty of Medicine, University of Toronto, Toronto, ON M5S 1A8, Canada, [c]Biology Department, Brookhaven National Laboratory, Upton, NY 11973-5000, USA, and [d]Department of Microbiology, University of Washington, Seattle, WA 98195-7735, USA

Correspondence e-mail: howell@sickkids.ca

Received 23 September 2011
Accepted 2 December 2011

The production of the PEL polysaccharide in *Pseudomonas aeruginosa* requires the binding of bis-(3′,5′)-cyclic dimeric guanosine monophosphate (c-di-GMP) to the cytoplasmic GGDEF domain of the inner membrane protein PelD. Here, the overexpression, purification and crystallization of a soluble construct of PelD that encompasses the GGDEF domain and a predicted GAF domain is reported. Diffraction-quality crystals were grown using the hanging-drop vapour-diffusion method. The crystals grew as flat plates, with unit-cell parameters $a = 88.3$, $b = 114.0$, $c = 61.9$ Å, $\alpha = \beta = \gamma = 90.0^\circ$. The PelD crystals exhibited the symmetry of space group $P2_12_12$ and diffracted to a minimum d-spacing of 2.2 Å. On the basis of the Matthews coefficient ($V_M = 2.29$ Å^3 Da^{-1}), it was estimated that two molecules are present in the asymmetric unit.

1. Introduction

Pseudomonas aeruginosa is a Gram-negative bacterium that can readily adapt to a variety of environmental conditions (Stover *et al.*, 2000). The preferred mode of growth of *P. aeruginosa* is in a densely populated multi-cellular community called a biofilm, a state in which the bacteria are encapsulated in a matrix that serves to protect the bacteria from host defences and provides resistance to antibiotics (Ryder *et al.*, 2007). The matrix is composed of exopolysaccharides, proteins and nucleic acids (Allesen-Holm *et al.*, 2006; Friedman & Kolter, 2004*a*).

P. aeruginosa is capable of forming three different types of exopolysaccharides encoded by three separate gene clusters: alginate, Psl and Pel (Ohman, 1986; Friedman & Kolter, 2004*b*; Jackson *et al.*, 2004; Stover *et al.*, 2000). Expression of the *pel* gene cluster has been linked to biofilm growth (Colvin *et al.*, 2011). Pel was discovered by screening a transposon mutant library for the lack of a specific type of biofilm which forms at the air–liquid interface of a standing culture and is known as a pellicle (Friedman & Kolter, 2004*b*). The genetic locus responsible for this phenotype has been identified and annotated as the *pelABCDEFG* operon (Friedman & Kolter, 2004*b*). While the composition of the pellicle remains mostly unknown, the matrix material may contain the O-antigen of lipopolysaccharide and cyclic glucans in addition to the Pel polysaccharide (Coulon *et al.*, 2010). Carbohydrate and linkage analyses suggest that the Pel polysaccharide is rich in glucose (Friedman & Kolter, 2004*b*).

The protein product of the *pelD* gene, PelD, has been identified as an essential regulator of pellicle formation and thus has been proposed as a possible target for therapeutic intervention (Lee *et al.*, 2007). PelD is a 51 kDa putative inner membrane protein which was predicted using the *Phyre*[2] server (Kelley & Sternberg, 2009) to contain four transmembrane (TM) helices at the N-terminus followed by tandem-arranged cytoplasmic GAF and GGDEF domains (Fig. 1*a*).

Studies in the last decade on the bacterial secondary messenger bis-(3′,5′)-cyclic dimeric guanosine monophosphate (c-di-GMP) have significantly increased our understanding of bacterial signalling. This molecule has been shown to be involved in the transition from the planktonic state to the sessile biofilm state, with higher cellular

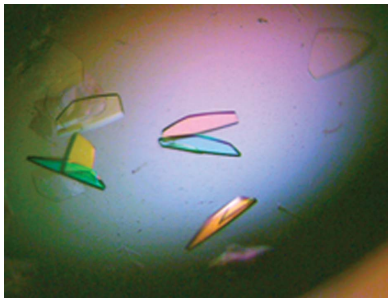

concentrations of c-di-GMP enhancing biofilm formation in multiple Gram-negative species (Tamayo *et al.*, 2007). Cyclic di-GMP receptors of known function are involved in exopolysaccharide synthesis, motility, transcription and subcellular or cell-surface protein localization (Schirmer & Jenal, 2009; Newell *et al.*, 2011). The formation of c-di-GMP is catalyzed by GGDEF-domain-containing diguanylate cyclases and is degraded by a family of enzymes called phosphodiesterases, which contain EAL or HD-GYP domains (Ryan *et al.*, 2006). GGDEF domains are named after the sequence of the amino acids that define the active site of diguanylate cyclases. These enzymes catalyze the formation of c-di-GMP through the cyclization of two guanosine triphosphate (GTP) molecules and are regulated by allosteric inhibition through the primary inhibition site (I_p site) characterized by the R*xx*D motif (De *et al.*, 2008). The GGDEF domain in PelD has been shown to be degenerate as it lacks the characteristic residues required for catalytic function, but the protein is still capable of binding c-di-GMP. Three conserved residues, Arg367, Asp370 and Arg402, thought to resemble the I_p site of the GGDEF domain found in *Caulobacter crescentus* PleD (Chan *et al.*, 2004) have been implicated in this binding and have been shown to be required for PEL polysaccharide production *in vivo*. These findings have led to the hypothesis that PelD acts as a c-di-GMP receptor and that c-di-GMP binding may provide a means of coupling PEL biosynthesis to export (Lee *et al.*, 2007).

PelD is also predicted to contain a GAF domain, a domain that has been implicated in a diverse array of functions (Aravind & Ponting, 1997). The name of this domain is derived from c**G**MP phosphodiesterases, **A**denylyl cyclases and **F**hlA, the first three protein families in which it was discovered. GAF domains are typically involved in ligand binding and/or protein–protein interactions; however, in bacteria GAF domains have also been shown to be associated with gene regulation (Aravind & Ponting, 1997). The role of the GAF domain in PelD has not yet been determined, but conceivably it could act as the signalling module and stimulate PEL production either through dimerization or possibly by interaction with one of the other Pel proteins in response to c-di-GMP binding.

To gain insight into the mechanism of PEL biosynthesis and export, and to determine the role of PelD in this process, we have initiated structural studies of PelD; here, we describe the overexpression, purification and crystallization of a soluble fragment of PelD encompassing the GAF and GGDEF domains.

2. Materials and methods

2.1. Cloning and expression

The nucleotide sequence of *pelD* from *P. aeruginosa* PA14 was obtained from the *Pseudomonas* Genome Database (Stover *et al.*, 2000) and was used to design primers specific to *pelD*. The forward primer, 5′-AAT CAT ATG AAC GAC CAG AGC CTG CGC AGT-3′, contains an *Nde*I restriction site, while the reverse primer, 5′-TCC CTC GAG CTA AAC AGC CAC TTG CTG ATC-3′,

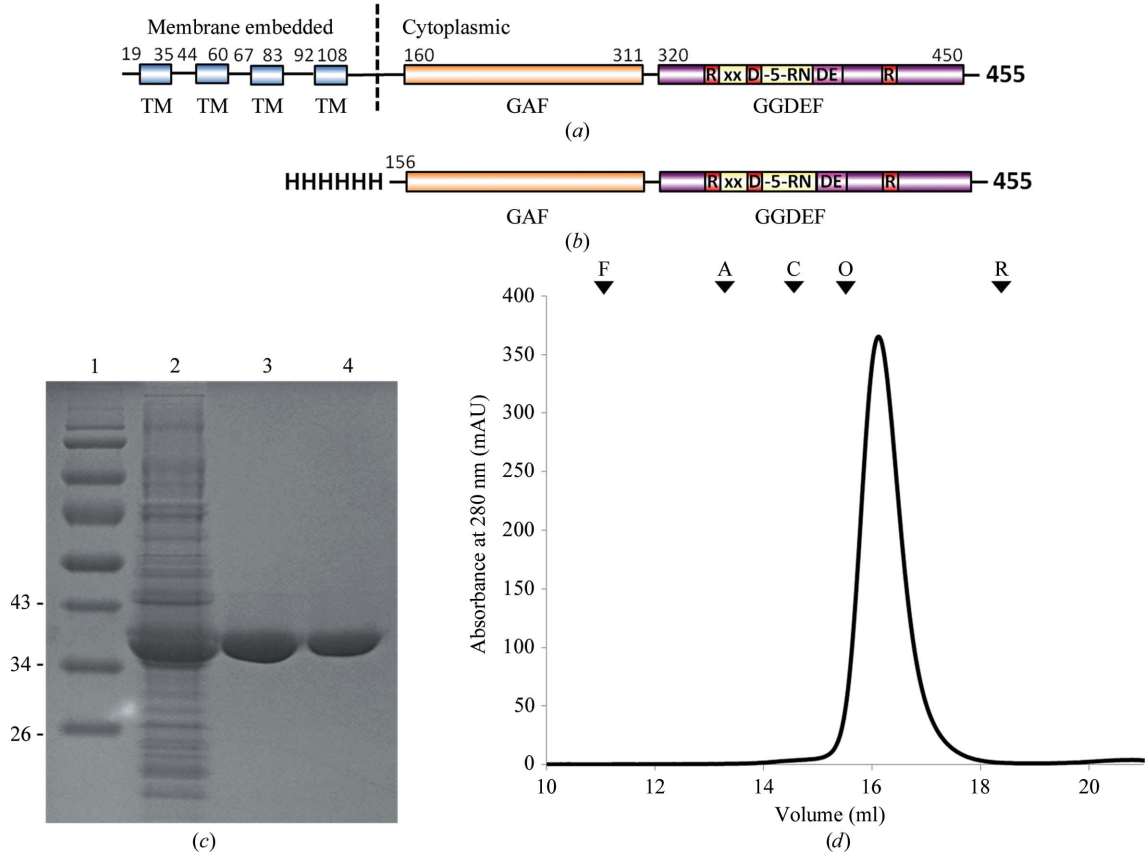

Figure 1
(*a*) Schematic diagram of the domain organization of PelD. The boundaries of the transmembrane (TM) segments and the GAF and GGDEF domains are denoted above the schematic and were predicted using *HMMTOP* (Tusnády & Simon, 2001) and *Phyre*[2] (Kelley & Sternberg, 2009), respectively. (*b*) Schematic diagram of the His_6-$PelD_{156–455}$ construct using in this study. (*c*) SDS–PAGE analysis of His_6-$PelD_{156–455}$ during expression and purification. Lane 1, molecular-weight markers (kDa); lane 2, soluble cell lysate; lane 3, purified His_6-$PelD_{156–455}$ after nickel-affinity chromatography; lane 4, following size-exclusion chromatography. (*d*) Size-exclusion chromatogram of His_6-$PelD_{156–455}$. Protein standards used to calibrate the column are indicated by inverted triangles; F, ferritin; A, aldolase; C, conalbumin; O, ovalbumin; R, ribonuclease A. The molecular weights of ferritin, aldolase, conalbumin, ovalbumin and ribonuclease A are 440, 158, 75, 43 and 13.7 kDa, respectively.

contains an *Xho*I restriction site. These primers were designed to generate a construct that included the predicted cytoplasmic GGDEF and GAF domains but excluded the predicted transmembrane secondary-structure elements. The amplified PCR products were digested with the *NdeI* and *Xho*I restriction endonucleases and were subsequently cloned into the pET28a vector (Novagen). Confirmation of the correct nucleotide sequence of *pelD* was achieved through DNA sequencing conducted by ACGT DNA Technologies Corporation. The resulting expression vector (pLSMPelD$_{156–455}$) encodes residues 156–455 of PelD fused to a cleavable N-terminal His$_6$ tag (His$_6$-PelD$_{156–455}$) for purification purposes (Fig. 1*b*).

Expression of PelD was achieved through the transformation of the PelD expression vector into *Escherichia coli* BL21 (DE3) competent cells, which were then grown in 2 l Luria–Bertani (LB) broth containing 50 µg ml^{-1} kanamycin at 310 K. The cells were grown to an OD$_{600}$ of 0.6, whereupon isopropyl β-D-1-thiogalactopyranoside (IPTG) was added to a final concentration of 1.0 m*M* to induce expression. The induced cells were incubated for 20 h at 298 K prior to being harvested *via* centrifugation at 6260*g* for 20 min at 277 K. The resulting cell pellet was stored at 253 K until required.

2.2. Purification

To purify the His$_6$-PelD$_{156–455}$ protein, the cell pellet from a 2 l bacterial culture was thawed and resuspended in 80 ml buffer *A* [50 m*M* Tris–HCl pH 8.0, 300 m*M* NaCl, 10%(*v*/*v*) glycerol, 1 m*M* tris(2-carboxyethyl)phosphine (TCEP)] containing one SIGMAFAST EDTA-free protease-inhibitor cocktail tablet (Sigma). Owing to the presence of four cysteines in PelD$_{156–455}$, TCEP was included to prevent intermolecular cross-linking of the protein. These cysteines are not suspected to be involved in disulfide-bond formation owing to their poor sequence conservation and the cytoplasmic localization of the native protein. The resuspension was then lysed by homogenization using an Emulsiflex-C3 (Avestin Inc.) at a pressure of between 69 and 103 MPa until the resuspension appeared translucent. Insoluble cell lysate was removed by centrifugation for 45 min at a speed of 25 000*g* at 277 K. The supernatant (Fig. 1*c*, lane 2) was loaded onto a 5 ml Ni^{2+}–NTA column pre-equilibrated with buffer *A* containing 5 m*M* imidazole to reduce background binding. To remove any contaminants, the column was washed with ten column volumes of buffer *A* containing 20 m*M* imidazole. Bound protein was eluted from the column with five column volumes of buffer *A* containing 250 m*M* imidazole. SDS–PAGE analysis revealed that the resulting His$_6$-PelD$_{156–455}$ was ∼95% pure and appeared at its expected molecular weight of 36 kDa (Fig. 1*c*, lane 3). Fractions containing PelD were pooled and concentrated to a volume of 2 ml by centrifugation at 2200*g* at a temperature of 277 K using an Amicon Ultra centrifugal filter device (Millipore) with a 30 kDa molecular-weight cutoff. PelD was further purified and buffer-exchanged into buffer *B* [20 m*M* Tris–HCl pH 8.0, 150 m*M* NaCl, 10%(*v*/*v*) glycerol, 1 m*M* DTT] by size-exclusion chromatography on a HiLoad 16/60 Superdex 200 gel-filtration column (GE Healthcare). PelD eluted as a single Gaussian-shaped peak (Fig. 1*d*); all PelD-containing fractions were pooled and the protein was concentrated by centrifugation at 2200*g* at a temperature of 277 K using an Amicon Ultra centrifugal filter device (Millipore) with a 30 kDa molecular-weight cutoff and stored at 277 K at a concentration of 10 mg ml^{-1} (Fig. 1*c*, lane 4). PelD could be stored in this manner for up to two months and retain its ability to form crystals. However, the solubility of PelD appears to be temperature-dependent. When the sample is exposed to temperatures of 277 K or below the sample becomes translucent as the protein precipitates. At temperatures above 277 K the sample returns to its original state with no observable detrimental effects to the protein sample or its crystallizability.

2.3. Crystallization

Commercial sparse-matrix crystal screens from Hampton Research and Emerald BioSystems were prepared at room temperature (295 K) using PelD at a concentration of 10 mg ml^{-1}. Trials were set up in 48-well VDX plates (Hampton Research) by hand with 3 µl drops consisting of a 1:1 ratio of protein and crystallization solution over a reservoir containing 250 µl crystallization solution. Crystal trays were stored at 295 K. Many hits were observed, particularly in conditions containing medium to high concentrations of polyethylene glycol (PEG). The best crystals were obtained from condition No. 43 [10%(*w*/*v*) PEG 8000, 100 m*M* Tris–HCl pH 7.0, 200 m*M* $MgCl_2$] of Wizard 2 (Emerald BioSystems). This condition yielded crystals which grew as flat plates with sharp edges that took approximately 5 d to grow to maximum dimensions of 200 × 400 × 75 µm (Fig. 2*a*). Optimization of this condition through adjustment of the precipitant concentration and buffer pH resulted in fewer nucleation sites and yielded crystals of identical size and morphology (Fig. 2*b*). Crystals of diffraction quality were able to form in a range of precipitant con-

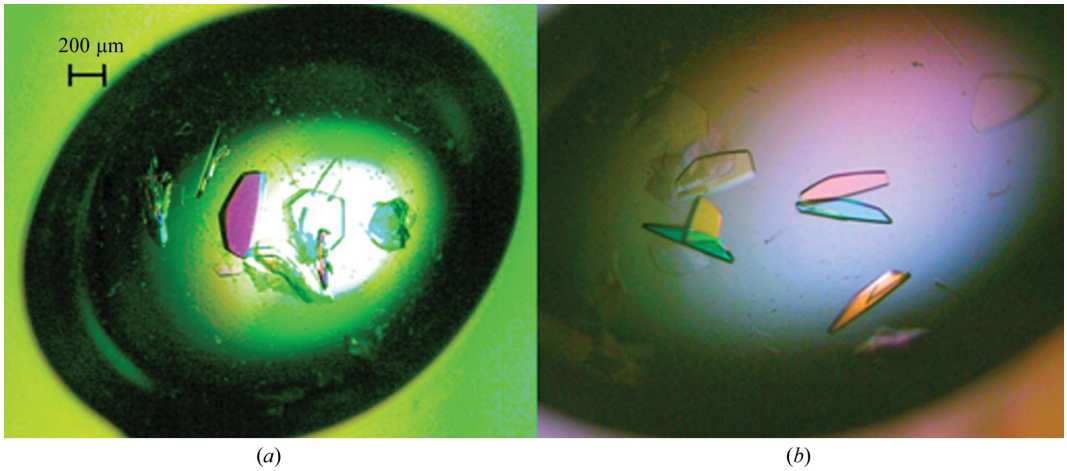

(*a*) (*b*)

Figure 2
Crystals of His$_6$-PelD$_{156–455}$. (*a*) Initial crystals grown from Wizard 2 condition No. 43 and (*b*) crystals obtained after optimization. The optimized crystals were grown in 11.5%(*w*/*v*) PEG 8000, 100 m*M* Tris–HCl pH 7.5, 200 m*M* $MgCl_2$.

Table 1
Data-collection statistics.

Values in parentheses are for the highest resolution shell.

Wavelength (Å)	1.075
Temperature (K)	100
Space group†	$P2_12_12$
Unit-cell parameters (Å, °)	a = 88.3, b = 114.0, c = 61.9, $\alpha = \beta = \gamma$ = 90.0
Resolution (Å)	50.00–2.20 (2.28–2.20)
Total No. of reflections	448882
No. of unique reflections	30063
Multiplicity	14.9 (7.5)
Completeness (%)	100.0 (100.0)
Average $I/\sigma(I)$	34.5 (5.4)
$R_{\rm merge}$‡ (%)	0.080 (0.53)

† The presence of a twofold axis along c was verified using *phenix.xtriage* and by manual inspection of the 00l reflections. ‡ $R_{\rm merge} = \sum_{hkl}\sum_i |I_i(hkl) - \langle I(hkl)\rangle|/\sum_{hkl}\sum_i I_i(hkl)$, where $I_i(hkl)$ and $\langle I(hkl)\rangle$ represent the diffraction-intensity values of the individual measurements and the corresponding mean values, respectively.

centrations [9.0–11.5%(*w*/*v*) PEG 8000] and pH (100 m*M* Tris–HCl pH 7.0–8.0). Crystals did not grow in the absence of $MgCl_2$, and alteration of the $MgCl_2$ concentration only decreased crystal quality.

2.4. Data collection

Prior to data collection, crystals were cryoprotected in well solution containing 20%(*v*/*v*) ethylene glycol added directly to the drop. Crystals were soaked in this solution for 10–15 s prior to vitrification in liquid nitrogen and were subsequently stored until X-ray diffraction data were collected on beamline X29A at the National Synchrotron Light Source (NSLS) at Brookhaven National Laboratory. A total of 360 images of 1° $\Delta\varphi$ oscillation were collected on an ADSC Q315 CCD detector with a 260 mm crystal-to-detector distance and an exposure time of 0.5 s per image. The data were processed using *DENZO* and integrated intensities were scaled using *SCALEPACK* from the *HKL*-2000 program package (Otwinowski & Minor, 1997). The data-collection statistics are summarized in Table 1.

3. Results

The cytoplasmic region of the putative inner membrane protein from *P. aeruginosa*, $PelD_{156–455}$, has been expressed and purified to near-homogeneity (∼99%; Fig. 1). Approximately 20 mg of purified His_6-$PelD_{156–455}$ could routinely be obtained per litre of cell culture. Diffraction-quality crystals have been grown and optimized. The crystals diffracted to 2.2 Å resolution and exhibited the symmetry of space group $P2_12_12$, with unit-cell parameters a = 88.3, b = 114.0, c = 61.9 Å, $\alpha = \beta = \gamma = 90.0°$. Based on density calculations, each asymmetric unit is predicted to contain two monomers of His_6-$PelD_{156–455}$ ($V_{\rm M}$ = 2.29 Å^3 Da^{-1}), with a calculated solvent content of 46.3% (Matthews, 1968). We are currently in the process of determining the structure of PelD using selenomethionine incorporation and the anomalous dispersion technique (Hendrickson, 1991).

The authors thank the ACGT DNA Technologies Corporation for assistance with DNA sequencing. This work was supported by research grants from the Canadian Institutes of Health Research to PLH (CIHR No. MT 43998) and from the National Institutes of Health (NIH; R01 AI077628-01A1) and National Science Foundation (NSF; MCB0822405) to MRP. PLH is the recipient of a Canada Research Chair. JCW has been supported by graduate scholarships from the Natural Sciences and Engineering Research Council of Canada, the Canadian Cystic Fibrosis Foundation, the Ontario Graduate Scholarship Program, the Ontario Student Opportunities Trust Fund and The Hospital for Sick Children Foundation Student Scholarship Program. Beamline X29 at the National Synchrotron Light Source, Brookhaven National Laboratory is supported by the Department of Energy and by a grant from the NIH National Centre for Research Resources.

References

Allesen-Holm, M., Barken, K. B., Yang, L., Klausen, M., Webb, J. S., Kjelleberg, S., Molin, S., Givskov, M. & Tolker-Nielsen, T. (2006). *Mol. Microbiol.* **59**, 1114–1128.
Aravind, L. & Ponting, C. P. (1997). *Trends Biochem. Sci.* **22**, 458–459.
Chan, C., Paul, R., Samoray, D., Amiot, N. C., Giese, B., Jenal, U. & Schirmer, T. (2004). *Proc. Natl Acad. Sci. USA*, **101**, 17084–17089.
Colvin, K. M., Gordon, V. D., Murakami, K., Borlee, B. R., Wozniak, D. J., Wong, G. C. L. & Parsek, M. R. (2011). *PLoS Pathog.* **7**, e1001264.
Coulon, C., Vinogradov, E., Filloux, A. & Sadovskaya, I. (2010). *PLoS One*, **5**, e14220.
De, N., Pirruccello, M., Krasteva, P. V., Bae, N., Raghavan, R. V. & Sondermann, H. (2008). *PLoS Biol.* **6**, e67.
Friedman, L. & Kolter, R. (2004*a*). *J. Bacteriol.* **186**, 4457–4465.
Friedman, L. & Kolter, R. (2004*b*). *Mol. Microbiol.* **51**, 675–690.
Hendrickson, W. A. (1991). *Science*, **254**, 51–58.
Jackson, K. D., Starkey, M., Kremer, S., Parsek, M. R. & Wozniak, D. J. (2004). *J. Bacteriol.* **186**, 4466–4475.
Kelley, L. A. & Sternberg, M. J. (2009). *Nature Protoc.* **4**, 363–371.
Lee, V. T., Matewish, J. M., Kessler, J. L., Hyodo, M., Hayakawa, Y. & Lory, S. (2007). *Mol. Microbiol.* **65**, 1474–1484.
Matthews, B. W. (1968). *J. Mol. Biol.* **33**, 491–497.
Newell, P. D., Boyd, C. D., Sondermann, H. & O'Toole, G. A. (2011). *PLoS Biol.* **9**, e1000587.
Ohman, D. E. (1986). *Eur. J. Clin. Microbiol.* **5**, 6–10.
Otwinowski, Z. & Minor, W. (1997). *Methods Enzymol.* **276**, 307–326.
Ryan, R. P., Fouhy, Y., Lucey, J. F., Crossman, L. C., Spiro, S., He, Y.-W., Zhang, L.-H., Heeb, S., Cámara, M., Williams, P. & Dow, J. M. (2006). *Proc. Natl Acad. Sci. USA*, **103**, 6712–6717.
Ryder, C., Byrd, M. & Wozniak, D. J. (2007). *Curr. Opin. Microbiol.* **10**, 644–648.
Schirmer, T. & Jenal, U. (2009). *Nat. Rev. Microbiol.* **7**, 724–735.
Stover, C. K. *et al.* (2000). *Nature (London)*, **406**, 959–964.
Tamayo, R., Pratt, J. T. & Camilli, A. (2009). *Annu. Rev. Microbiol.* **61**, 131–148.
Tusnády, G. E. & Simon, I. (2001). *Bioinformatics*, **17**, 849–850.